

# Homocalixpyridines: Ligands Exhibiting High Selectivity in Extraction and Sensor Processes

Holger Stephan, Torsten Krüger-Rambusch, Karsten Gloe,\* Wolfgang Hasse, Benedikt Ahlers, Karl Cammann, Kari Rissanen, Gisela Brodesser, and Fritz Vögtle\*

**Abstract:** A series of differently functionalised *all*-homocalixpyridines **I** and their open-chain analogues **II** were synthesised by use of the Müller–Röscheisen reaction. Their complexation properties were then investigated by extraction and liquid membrane experiments. This new class of macrocycles composed of pyridine units shows a pronounced selectivity towards soft metal ions, such as Ag<sup>I</sup>, Pd<sup>II</sup>, Hg<sup>II</sup> and Au<sup>III</sup>. The complexation behaviour can be easily modified by variation of the ring size and substitution pattern. Molecular modelling studies of the ligands, as well as their silver(I) and mercury(II) complexes, were performed in order to understand the principles of complex formation. Furthermore, the use of the new ligands as ionophores in PVC-based membrane electrodes was studied.

**Keywords:** homocalixarenes • host–guest chemistry • mercury • molecular modeling • silver

## Introduction

By developing homocalixarenes,<sup>[1]</sup> which exhibit a stable hydrocarbon host skeleton based on [2<sub>n</sub>]metacyclophanes and which can have a variable ring size, we have paved the way for a versatile host architecture. The introduction of additional CH<sub>2</sub> groups in all the aliphatic bridges leads to a higher flexibility of these hosts compared with calixarenes,<sup>[2]</sup> and consequently stable conformations—which are unfavourable for the complexation of any guests—are avoided. The Müller–Röscheisen synthesis<sup>[3]</sup> was the method chosen for

the preparation, as it has the advantage of being able to directly add heteroaromatic units to the framework. The use of pyridine as a complexing unit in such systems offers interesting coordination possibilities towards metal ions owing to the polarity of the nitrogen donor atom and the orientation of the lone electron pair.<sup>[4]</sup> Although pyridine macrocycles with additional donor atoms, such as ether oxygen, amine nitrogen and thioether sulfur, have been developed as host compounds, this leads to rather poor separation selectivity for metal ions due to the multifunctional interactions of the macrocycles.<sup>[5]</sup>

Hitherto, the macrocyclic pyridine oligomers **3** (trimer) and **5** (pentamer) were isolated as the main products of the OCH<sub>3</sub>-substituted series.<sup>[6]</sup> In this work, we synthesised a series of macroheterocyclic oligomers **I** containing unsubstituted (**1, 2**), methoxy- (**3–6**) and methoxyethoxy-substituted (**7–10**) pyridine building blocks. For comparison, we also prepared the structurally analogous open-chain oligopyridines **II** (Figure 1).

Thus, we report on the tailoring of host molecules containing endobasic pyridine donor sites towards certain soft metal ions. By synthesising complete series of ligands, we were able to investigate the influence of the following parameters on the complexation behaviour:

- The ring size and the number of identical binding sites.
- Variation of the substituent in the 4-position of the pyridine unit and the consequent alteration in the donating capacity and lipophilicity of the homocalixpyridines **I**.
- Effect of the macrocyclic structure in comparison with the corresponding open-chain oligopyridines **II**.

[\*] Prof. Dr. K. Gloe, Dr. H. Stephan, Dipl.-Chem. T. Krüger-Rambusch  
Institut für Anorganische Chemie  
der Technischen Universität Dresden  
Mommensenstrasse 13, D-01062 Dresden (Germany)  
Fax: (+ 49) 351-463-7287  
E-mail: karsten.gloe@chemie.tu-dresden.de

Prof. Dr. F. Vögtle, Dr. G. Brodesser  
Institut für Organische Chemie und Biochemie der Universität Bonn  
Gerhard-Domagk-Strasse 1, D-53121 Bonn (Germany)  
Fax: (+ 49) 228-73-5662  
E-mail: voegt@uni-bonn.de

Prof. Dr. K. Cammann, Dr. Wolfgang Hasse, Dr. Benedikt Ahlers  
Institut für Chemo- und Biosensorik  
Mendelstrasse 11, D-48149 Münster (Germany)  
Fax: (+ 49) 251-980-1999

Prof. Dr. K. Rissanen  
University of Jyväskylä, Department of Organic Chemistry  
P.O. Box 35, Surfontie 9, Fin-40301 Jyväskylä (Finland)  
Fax: (+ 358) 41-60-2501  
E-mail: rissanen@jykem.jyu.fi

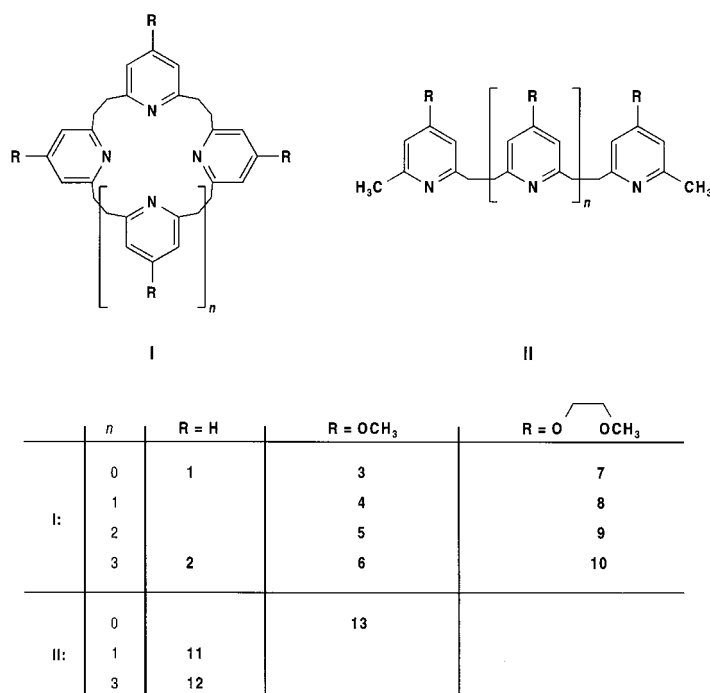


Figure 1. Synthesized *all*-homocalixpyridines and open-chain pyridine oligomers.

Solvent extraction and membrane studies were used as the experimental techniques and the results were interpreted by molecular modelling.

## Results and Discussion

Complexation behaviour was studied by means of extraction experiments in the system metal salt-buffer-H<sub>2</sub>O/homocalixpyridine-CHCl<sub>3</sub>.<sup>[7]</sup> The extractabilities of different metal ions with the *all*-homocalixpyridines **1**, **3** and **7**, which each contain three pyridine units inside the ring skeleton, are presented in Figure 2. In aqueous solutions containing nitrate, there was a pronounced selectivity for silver compared to the other metal ions investigated (Figure 2a). The extractabilities of Hg<sup>II</sup> and

**Abstract in German:** *Mit Hilfe der Müller-Röscheisen-Synthese wurden eine Reihe unterschiedlich funktionalisierter all-Homocalixpyridine I sowie strukturanaloger offenkettiger Liganden II hergestellt und hinsichtlich ihrer Komplexbildungseigenschaften gegenüber Metallionen durch Flüssig-Flüssig-Extraktions- sowie Flüssig-Membran-Untersuchungen charakterisiert. Diese neue Verbindungsklasse makrocyclischer pyridinhaltiger Komplexbildner weist eine hohe Selektivität für weiche Metallionen wie Ag<sup>I</sup>, Pd<sup>II</sup>, Hg<sup>II</sup> und Au<sup>III</sup> auf. Die Komplexbildungseigenschaften können in einfacher Weise durch Änderung der Ringgröße sowie durch Variation der Substituenten geändert werden. Zur Interpretation von Struktur-Wirkungsbeziehungen wurden Molecular Modeling-Rechnungen an den all-Homocalixpyridinen sowie ihren Ag<sup>I</sup>- und Hg<sup>II</sup>-Komplexen durchgeführt. Der Einsatz dieser neuen Liganden als Ionophore in PVC-Flüssig-Membran-Elektroden wurde untersucht.*

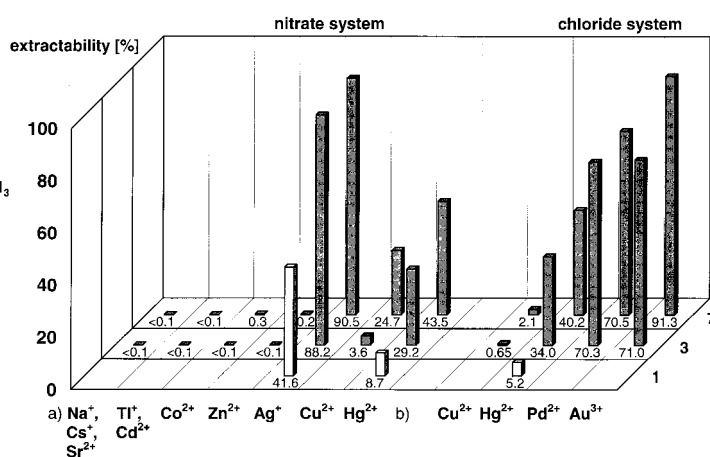


Figure 2. Extractability of different metal ions with *all*-homocalixpyridines **1**, **3** and **7**. a)  $[M(NO_3)_n] = 1 \times 10^{-4}$  M;  $[KNO_3] = 0.1$  M; pH = 6.3 (MES/NaOH buffer);  $[all\text{-homocalixpyridine}] = 1 \times 10^{-3}$  M in CHCl<sub>3</sub>. b)  $[MCl_n] = 1 \times 10^{-4}$  M (M = Cu<sup>2+</sup>, Pd<sup>2+</sup>); pH = 5.2 (NaOAc/HCl buffer);  $[HAuCl_4] = 1 \times 10^{-4}$  M;  $[HNO_3] = 1 \times 10^{-2}$  M;  $[all\text{-homocalixpyridine}] = 1 \times 10^{-3}$  M in CHCl<sub>3</sub>.

Cu<sup>II</sup> were remarkable lower than that of Ag<sup>I</sup>. The experiments demonstrate that in all cases 1:1 complexes with these metal cations dominate in organic solution.<sup>[8]</sup> There was negligible extraction of other transition metal ions, such as Co<sup>II</sup>, Zn<sup>II</sup> and Cd<sup>II</sup>. As expected, no interaction was found between the *all*-homocalixpyridines and hard metal ions, such as those of alkali and alkaline earth metals.

The extraction efficiency and selectivity of homocalixpyridines depend strongly on the substitution pattern of the pyridine rings. Thus, the unsubstituted *all*-homocalix[3]pyridine **1** (R = H) exhibited a lower efficiency for Ag<sup>I</sup> and Hg<sup>II</sup> compared to the substituted ligands **3** and **7** with the same ring size, but with an additional substituent (**3**: R = OCH<sub>3</sub>, **7**: R = OCH<sub>2</sub>CH<sub>2</sub>OCH<sub>3</sub>).

Molecular modelling calculations of the ligand–metal ion interactions for Ag<sup>I</sup> and Hg<sup>II</sup> in the extracted 1:1 complexes allow the interpretation of this finding (Figure 3).<sup>[9]</sup> Thus, the arrangement of both ions is clearly improved on going from ligand **1** to **3** to **7**. Retaining the partial cone conformation found as the energy optimum of the free ligands, the metal–pyridine nitrogen donor atom distances for the 1:1 complexes calculated are significantly lowered for **3** and **7** compared with **1**. This could be explained on the one hand by electronic effects on the basicity of the nitrogen atom,<sup>[10]</sup> but also by the participation of an ether oxygen atom from a side chain on the formation of the complex (Figure 3, lower structures). Furthermore, it is interesting that the binding distances for the silver(I) complexes in all three examples are much shorter than those of the corresponding mercury(II) complexes. As shown in Figure 3, the silver ion is more deeply embedded in the calix formed. This result correlates very well with the experimentally observed order of graduated extractability given in Figure 2a: the extractability of Ag<sup>I</sup> is greater than that of Hg<sup>II</sup>.

Soft metal ions were also extracted from solutions containing chloride with high efficiency. An effective separation of noble metal ions, such as Pd<sup>II</sup> and Au<sup>III</sup>, from such solutions was possible (Figure 2b). The remarkable selectivity of Pd<sup>II</sup>

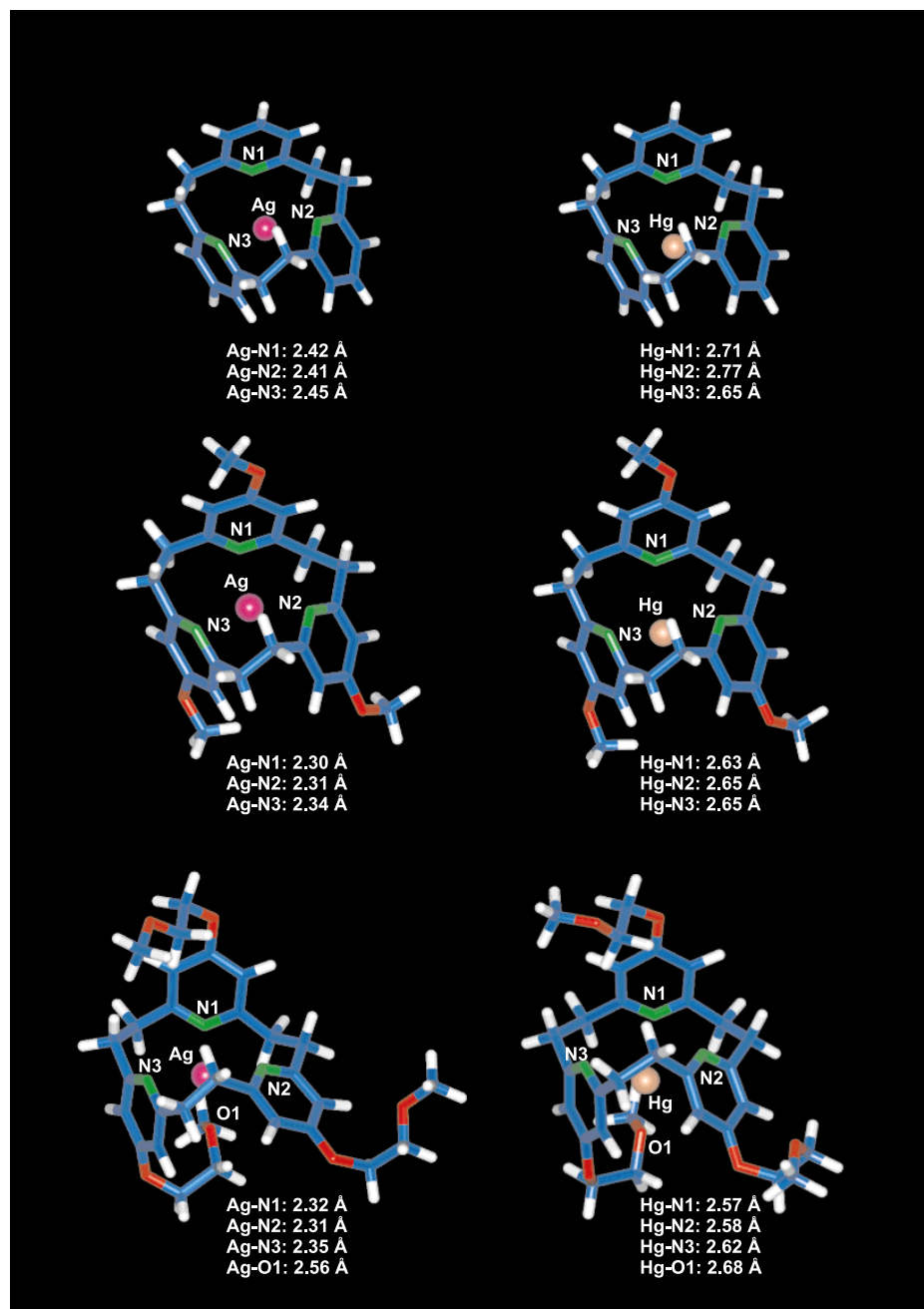


Figure 3. Molecular modelling of the  $\text{AgL}^+$  (left) and  $\text{HgL}^{2+}$  complexes (right) with **1**, **3** and **7** (from the top to the bottom) by DFT calculations.

and  $\text{Au}^{\text{III}}$  over  $\text{Cu}^{\text{II}}$  is interesting in view of a selective removal of these noble metals from effluents.

The interpretation of the extraction data for cyclic and open-chain derivatives with a varying number of pyridine units is more complicated than the influence of substitution. Generally, the counteranion and the pH of the aqueous phase strongly influenced the extraction properties.<sup>[11]</sup>

The results of  $\text{Ag}^{\text{I}}$ ,  $\text{Hg}^{\text{II}}$  and  $\text{Cu}^{\text{II}}$  extraction differ depending on both the ligand and the aqueous system used (Figure 4). For  $\text{Ag}^{\text{I}}$ , the extractabilities of **4**–**6** are high and there is only a small difference on changing the number of pyridine units in the molecule. For  $\text{Hg}^{\text{II}}$  and  $\text{Cu}^{\text{II}}$ , the highest extractability from nitrate solution was achieved with **6**, the macrocycle with six pyridine units, whereas **4** and **5**, in particular, extracted

$\text{Hg}^{\text{II}}$  from chloride solution with high efficiency and selectivity over  $\text{Cu}^{\text{II}}$ . The reasons for this behaviour are not yet clear. Probably differences in the structure of the extracted complexes play an important role. Obviously, an optimum arrangement of the linear  $\text{HgCl}_2$  species, which is extracted from chloride solution, is only possible in the case of compounds **4** and **5**.

The benefit of the cyclisation step on complex formation is expressed by the differences between the extractabilities of the homocalixpyridines **I** and the open-chain oligopyridines **II**. As shown in Figures 2 and 4, the comparison of extraction behaviour in the nitrate system for the compounds **1**, **3** and **11** with three pyridine units and **5** and **12** with five pyridine units reveals that the open-chain ligands are less efficient for  $\text{Ag}^{\text{I}}$  extraction (**1**: 42%; **3**: 88%; **11**: 26% and **5**: 99%; **12**: 44%), and less selective for  $\text{Ag}^{\text{I}}$ / $\text{Hg}^{\text{II}}$  separation than the macrocyclic compounds (**1**:  $\text{Ag}^{\text{I}}$  42%,  $\text{Hg}^{\text{II}}$  9%; **3**:  $\text{Ag}^{\text{I}}$  88%,  $\text{Hg}^{\text{II}}$  29%; **11**:  $\text{Ag}^{\text{I}}$  26%,  $\text{Hg}^{\text{II}}$  20% and **5**:  $\text{Ag}^{\text{I}}$  99%,  $\text{Hg}^{\text{II}}$  39%; **12**:  $\text{Ag}^{\text{I}}$  44%,  $\text{Hg}^{\text{II}}$  59%). The most favourable separation selectivity for the macrocycles is achieved by the trimer **3**, which is the main product of the Müller–Röscheisen synthesis. Nevertheless, the open-chain bispyridine derivative **13** also gave a significant preference of  $\text{Ag}^{\text{I}}$  over  $\text{Hg}^{\text{II}}$ .

It is interesting to note that the results for  $\text{Hg}^{\text{II}}$  are slightly modified in comparison to  $\text{Ag}^{\text{I}}$ , although size and coordination behaviour of both are similar. Thus, a remarkable extraction power for  $\text{Hg}^{\text{II}}$  was observed with the open-chain compounds **12** (59%) from nitrate- and **13** (63%) from chloride-containing solutions. In particular, the results for  $\text{Hg}^{\text{II}}$  extraction with the open-chain pyridine compounds in a nitrate solution are quite different from those in a chloride medium. While the order of increasing extractability from nitrate solutions (**13** < **11** < **12**) correlates with  $\text{Ag}^{\text{I}}$ , the order for chloride solutions is different (**11** < **12** < **13**). In this last case the bidentate ligand **13** obviously allows the favourable coordination number 4 for  $\text{Hg}^{\text{II}}$  by forming a 1:1 complex with  $\text{HgCl}_2$ . This observation is in good agreement with solvent extraction data of various open-chain ligands containing N, S and O.<sup>[12]</sup>

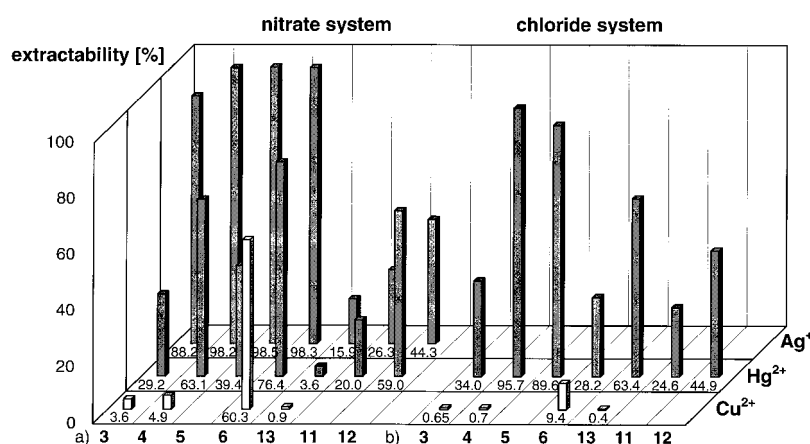


Figure 4. Extractability of  $\text{Cu}^{2+}$ ,  $\text{Hg}^{2+}$  and  $\text{Ag}^+$  with all-homocalixpyridines **3**–**6** and pyridine oligomers **11**–**13** (experimental conditions are the same as in Figure 2).

The protonation of the pyridine nitrogen, which would cause the blocking of the donor sites, must also be considered in the discussion of the experimental results. Thus, the efficiency of metal extraction with pyridine-containing ligands is considerably influenced by a change of pH. A typical trend of  $\text{Ag}^+$  extraction with the macrocycle **5** as a function of pH in nitrate solution is shown in Figure 5. As expected, the

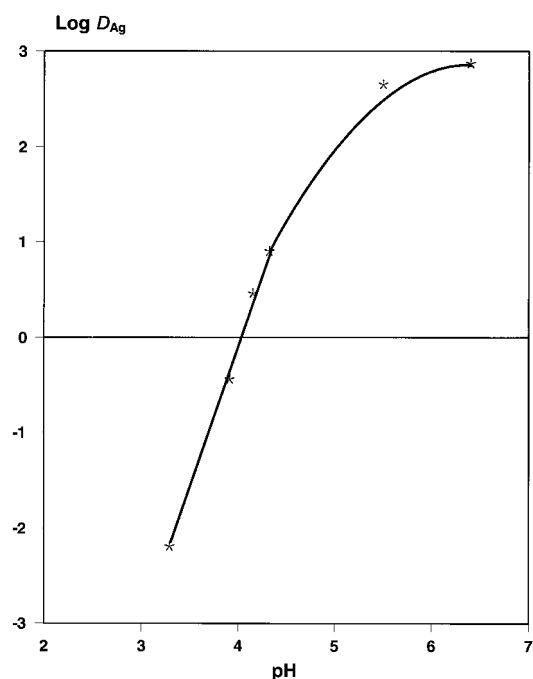


Figure 5. Extraction of  $\text{Ag}^+$  with **5** as a function of pH.  $[\text{AgNO}_3] = 1 \times 10^{-4} \text{ M}$ ,  $[\text{KNO}_3] = 1.1 \text{ M}$ ,  $\text{pH} = 3.3$ – $6.3$  (variation by  $\text{HNO}_3$ ).

distribution ratios increased with rising pH due to the deprotonation of the pyridine nitrogen. Above pH 6, the distribution ratio is constant because the ligand is mainly deprotonated ( $\text{p}K_{\text{a}(\text{pyridine})} = 5.25$ ). Therefore, the extraction efficiency and separation selectivity for different metal ions can be governed by a defined protonation of the ligands. On the other hand, the back extraction of metal ions is possible by

decreasing the pH. In our experiments, the pH values were different for the nitrate and chloride media, and were controlled by various buffer solutions.

In contrast to the results for  $\text{Ag}^+$  in solution, which indicated the formation of a 1:1 complex, a solid multinuclear silver complex of trimer **3** was isolated from a dichloromethane/acetonitrile mixture. The complex was identified as a trinuclear silver tetrafluoroborate containing the  $[(\text{Ag}^+)_3(\text{CH}_3\text{CN})_3(\mathbf{3})]^{3+}$  cation.<sup>[13]</sup> The X-ray structure analysis (Figure 6) revealed that the partial cone conformation of the free ligand<sup>[6]</sup> is preserved and each pyridine nitrogen binds one  $\text{Ag}^+$  cation to form a trinuclear complex, the second binding site of the linearly coordinated silver is occupied by an acetonitrile molecule.<sup>[14]</sup> To our knowledge, such a nearly linear arrangement  $\text{Py-Ag-CH}_3\text{CN}$  was unknown until now.<sup>[15]</sup> The  $\text{Ag1-Ag2}$  distance is 390.8 pm, which is shorter than the sum of the van der Waals radii.<sup>[16]</sup>

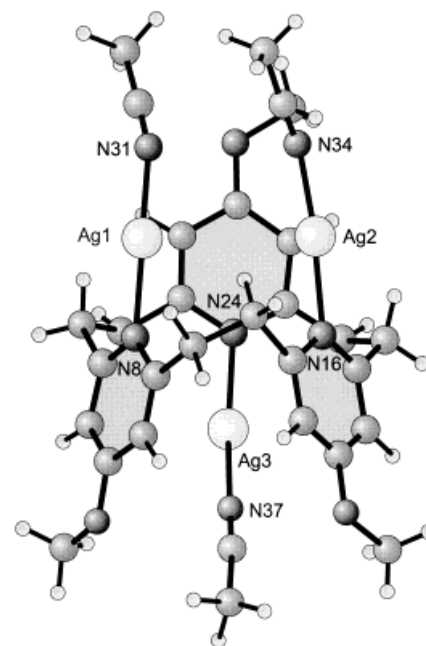


Figure 6. X-ray crystal structure of the trinuclear complex ion  $[(\text{Ag}^+)_3(\text{CH}_3\text{CN})_3(\mathbf{3})]$ .

In order to test the ionophore properties of the novel homocalixpyridines, PVC-based membrane electrodes and transport experiments were performed. The results obtained show that the compounds are suitable as ionophores for liquid membrane electrodes and as carriers mediating the transport of silver ions through bulk liquid membranes.<sup>[7,17]</sup> The selective interaction of silver ions with compounds **1**–**7** was confirmed by potentiometric measurements carried out after the addition of an anion blocker into the membrane. Thus, the anion interference was suppressed and the permselectivity for silver ions was measured. The response times of the electrodes with **1**–**7** are in the range of few seconds, the detection limits

( $10^{-4.5}$ – $10^{-5.3}$  M) are very low, and the slope with 56–59 mV decade<sup>-1</sup> is almost optimal. Figure 7 shows the selectivity coefficients for PVC membrane electrodes given as  $\log K_{ij}^{\text{pot}}$  of  $\text{Ag}^+$  and  $\text{Tl}^+$  for **3** and **7**. The preference for silver is not influenced by the ring size of the macrocycles. In contrast to this, the introduction of side arms (**3**→**7**) leads to a change in the selectivity from  $\text{Ag}^+$  to  $\text{Tl}^+$ .

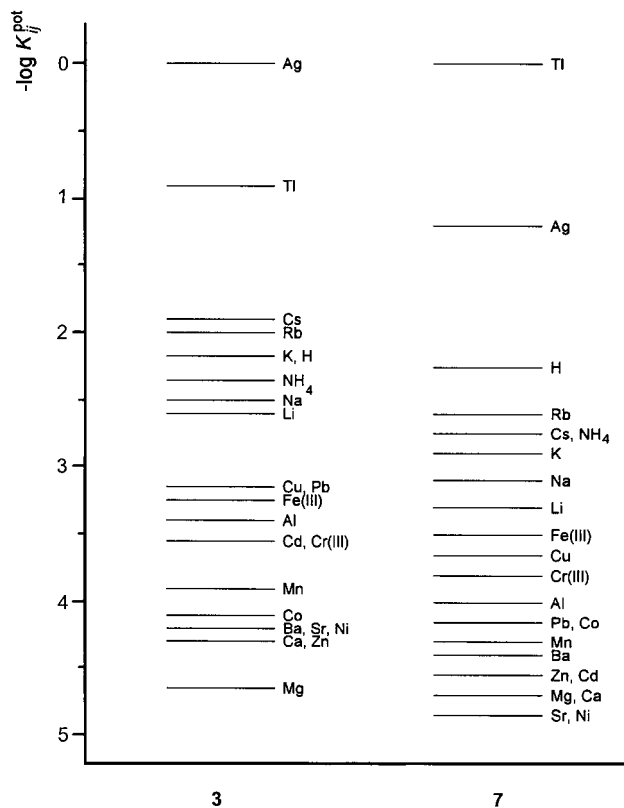


Figure 7. Selectivity coefficients for membrane electrodes containing carrier **3** and **7**.

The transport properties of selected homocalixpyridines **3**, **5** and **7** for a variety of ions have been proved using a liquid membrane system source phase ( $5 \times 10^{-2}$  M  $\text{Ag}^+$ ,  $5 \times 10^{-2}$  M  $\text{M}^{n+}$ , nitrate)/membrane ( $5 \times 10^{-4}$  M in  $\text{CHCl}_3$ )/receiving phase ( $\text{H}_2\text{O}$ ). A high selectivity for  $\text{Ag}^+$  over  $\text{Na}^+$ ,  $\text{K}^+$ ,  $\text{Tl}^+$ ,  $\text{Pb}^{\text{II}}$ ,  $\text{Cu}^{\text{II}}$  and  $\text{Hg}^{\text{II}}$  was observed for the carriers investigated. The ion flux for  $\text{Ag}^+$  in single ion-transport experiments was determined as  $3.2 \times 10^{-3} \text{ mol m}^{-2} \text{ h}^{-1}$  (**3**),  $7.8 \times 10^{-3} \text{ mol m}^{-2} \text{ h}^{-1}$  (**5**) and  $7.7 \times 10^{-3} \text{ mol m}^{-2} \text{ h}^{-1}$  (**7**). Thus, the ion flux is improved by both the introduction of side arms (**3**→**7**) and the increase of binding sites (**3**→**5**). The results obtained for transport experiments are in good agreement with the liquid–liquid extraction data.

## Experimental Section

**General:**  $^1\text{H}$  NMR spectra were recorded on a Varian EM360 (60 MHz) and Bruker AC200 (200 MHz), WM250 (250 MHz), AM400 (400 MHz) spectrometers.  $^{13}\text{C}$  NMR spectra were recorded on Bruker AC200 (200 MHz) and AM400 (400 MHz) spectrometers. FAB mass spectra were obtained with a Kratos Concept 1H (3-nitrobenzyl alcohol as a matrix).

Chromatography separations were performed on silica gel 60 ( $\text{SiO}_2$ , Merck, particle size: 0.040–0.063 mm). HPLC separations were carried out on a Abimed-Gilson pump 305/306 with a Lichrosorb Si-60-5 (250 × 8 mm) column, Chromatographie Service GmbH and a Gilson holochrome detector.

**General procedure for the preparation of all-homocalix[n](2,6)pyridines:** Powdered sodium (400 mmol) and tetraphenylethene (TPE, 9 mmol) were stirred under Ar in dry THF (1 L) for 3 h at room temperature, whereby the reaction mixture turned deep red. After stirring at  $-90^\circ\text{C}$ , a solution of the corresponding bis(bromomethyl) compound (40 mmol) in dry THF (250 mL) was added dropwise through a perfusor over a period of 12 d and the solution remained red. The mixture was treated with methanol (1 mL) and the colour changed from red to yellow. After warming to RT, excess sodium was filtered off and the residue carefully washed with THF. The reaction mixture was treated once more with methanol to be sure all the sodium had been removed, and the solvent then evaporated. The residue was taken up with trichloromethane (250 mL) and refluxed for 1 h. The inorganic solid was filtered off and the solvent evaporated. The crude product was subjected to column chromatography (silica gel,  $\text{CH}_2\text{Cl}_2$ ) to remove the unreacted TPE and the reaction products then completely eluted with methanol. Separation of homocalixpyridines was performed by column chromatography with  $\text{CH}_2\text{Cl}_2/\text{MeOH}/\text{conc NH}_3$  as the eluent [100:5:1 (**13**), 100:7.5:1 (**7**), 100:10:1 (**1**, **2**, **4**, **6**, **11**, **12**), 100:15:1 (**8**, **9**, **10**)]. Final purification was achieved by HPLC with  $\text{CH}_2\text{Cl}_2/\text{MeOH}/\text{conc NH}_3$  [82.5:17.5:0.5 (**4**, **6**), 90:10:1 (**8**, **9**, **10**)].

**all-Homocalix[3](2,6)pyridine (1):** Yield: 1%; yellow solidified oil; TLC ( $\text{SiO}_2$ ):  $R_f = 0.65$  ( $\text{CH}_2\text{Cl}_2/\text{MeOH}/\text{conc NH}_3$  100:10:1);  $^1\text{H}$  NMR (250 MHz,  $\text{CDCl}_3$ ,  $25^\circ\text{C}$ ):  $\delta = 2.98$  (s, 12H;  $\text{CH}_2$ ), 6.8 (d,  $^3J = 7.7$  Hz, 6H; Ar-H), 7.33 (t,  $^3J = 7.7$  Hz, 3H; Ar-H);  $^{13}\text{C}$  NMR (62.9 MHz,  $\text{CDCl}_3$ ,  $25^\circ\text{C}$ ):  $\delta = 159.65$  (C), 135.58 (CH), 120.15 (CH), 37.96 ( $\text{CH}_2$ ).

**all-Homocalix[6](2,6)pyridine (2):** Yield: 0.15%; yellow solidified oil; TLC ( $\text{SiO}_2$ ):  $R_f = 0.3$  ( $\text{CH}_2\text{Cl}_2/\text{MeOH}/\text{conc NH}_3$  100:10:1);  $^1\text{H}$  NMR (250 MHz,  $\text{CDCl}_3$ ,  $25^\circ\text{C}$ ):  $\delta = 3.15$  (s, 12H;  $\text{CH}_2$ ), 6.69 (d,  $^3J = 7.7$  Hz, 6H; Ar-H), 7.25 (t,  $^3J = 7.7$  Hz, 3H; Ar-H).

**6,13,20,27-Tetramethoxy-all-homocalix[4](2,6)pyridine (4):** Yield: 0.4%; m.p.  $195^\circ\text{C}$ ; TLC ( $\text{SiO}_2$ ):  $R_f = 0.4$  ( $\text{CH}_2\text{Cl}_2/\text{MeOH}/\text{conc NH}_3$  100:10:1);  $^1\text{H}$  NMR (250 MHz,  $\text{CDCl}_3$ ,  $25^\circ\text{C}$ ):  $\delta = 2.97$  (s, 16H;  $\text{CH}_2$ ), 3.68 (s, 12H;  $\text{OCH}_3$ ), 6.32 (s, 8H; Ar-H); MS (FAB):  $m/z$  (%) = 541.3 (100) [ $\text{M}^+ + \text{H}$ ].

**6,13,20,27,34,41-Hexamethoxy-all-homocalix[6](2,6)pyridine (6):** Yield: 0.4%; m.p.  $117^\circ\text{C}$ ; TLC ( $\text{SiO}_2$ ):  $R_f = 0.2$  ( $\text{CH}_2\text{Cl}_2/\text{MeOH}/\text{conc NH}_3$  100:10:1);  $^1\text{H}$  NMR (250 MHz,  $\text{CDCl}_3$ ,  $25^\circ\text{C}$ ):  $\delta = 3.07$  (s, 24H;  $\text{CH}_2$ ), 3.70 (s, 18H;  $\text{OCH}_3$ ), 6.46 (s, 12H; Ar-H);  $^{13}\text{C}$  NMR (22.63 MHz,  $\text{CDCl}_3$ ,  $25^\circ\text{C}$ ):  $\delta = 167.17$  (C), 161.21 (C), 107.11 (CH), 55.48 ( $\text{CH}_3$ ), 36.98 ( $\text{CH}_2$ ); MS (FAB):  $m/z$  (%) = 811.4 (100) [ $\text{M}^+ + \text{H}$ ].

**6,13,20-Tris(2-methoxyethoxy)-all-homocalix[3](2,6)pyridine (7):** Yield: 7%; colourless solidified oil; TLC ( $\text{SiO}_2$ ):  $R_f = 0.4$  ( $\text{CH}_2\text{Cl}_2/\text{MeOH}/\text{conc NH}_3$  100:15:1);  $^1\text{H}$  NMR (200 MHz,  $\text{CDCl}_3$ ,  $25^\circ\text{C}$ ):  $\delta = 2.99$  (s, 12H;  $\text{CH}_2$ ), 3.41 (s, 9H;  $\text{OCH}_3$ ), 3.69 (m, 6H;  $\text{CH}_2$ ), 4.10 (m, 6H;  $\text{CH}_2$ ), 6.41 (s, 6H; Ar-H);  $^{13}\text{C}$  NMR (100.61 MHz,  $\text{CDCl}_3$ ,  $25^\circ\text{C}$ ):  $\delta = 164.93$  (C), 161.16 (C), 106.73 (CH), 70.75 ( $\text{CH}_2$ ), 66.70 ( $\text{CH}_2$ ), 59.28 ( $\text{CH}_3$ ), 37.78 ( $\text{CH}_2$ ); MS (FAB):  $m/z$  (%) = 538.3 (100) [ $\text{M}^+ + \text{H}$ ].

**6,13,20,27-Tetrakis(2-methoxyethoxy)-all-homocalix[4](2,6)pyridine (8):** Yield: 0.3%; colourless solidified oil; TLC ( $\text{SiO}_2$ ):  $R_f = 0.6$  ( $\text{CH}_2\text{Cl}_2/\text{MeOH}/\text{conc NH}_3$  100:15:1);  $^1\text{H}$  NMR (400 MHz,  $\text{CDCl}_3$ ,  $25^\circ\text{C}$ ):  $\delta = 3.12$  (s, 16H;  $\text{CH}_2$ ), 3.41 (s, 12H;  $\text{OCH}_3$ ), 3.74 (m, 8H;  $\text{CH}_2$ ), 4.25 (m, 8H;  $\text{CH}_2$ ), 6.82 (s, 8H; Ar-H);  $^{13}\text{C}$  NMR (100.61 MHz,  $\text{CDCl}_3$ ,  $25^\circ\text{C}$ ):  $\delta = 167.51$  (C), 160.34 (C), 108.2 (CH), 70.42 ( $\text{CH}_2$ ), 67.94 ( $\text{CH}_2$ ), 59.14 ( $\text{CH}_3$ ), 36.94 ( $\text{CH}_2$ ); MS (FAB):  $m/z$  (%) = 717.3 (100) [ $\text{M}^+ + \text{H}$ ].

**6,13,20,27,34-Pentakis(2-methoxyethoxy)-all-homocalix[5](2,6)pyridine (9):** Yield: 0.4%; colourless solidified oil; TLC ( $\text{SiO}_2$ ):  $R_f = 0.55$  ( $\text{CH}_2\text{Cl}_2/\text{MeOH}/\text{conc NH}_3$  100:15:1);  $^1\text{H}$  NMR (400 MHz,  $\text{CDCl}_3$ ,  $25^\circ\text{C}$ ):  $\delta = 3.1$  (s, 20H;  $\text{CH}_2$ ), 3.4 (s, 15H;  $\text{OCH}_3$ ), 3.74 (m, 10H;  $\text{CH}_2$ ), 4.25 (m, 10H;  $\text{CH}_2$ ), 6.77 (s, 10H; Ar-H);  $^{13}\text{C}$  NMR (100.61 MHz,  $\text{CDCl}_3$ ,  $25^\circ\text{C}$ ):  $\delta = 166.96$  (C), 160.74 (C), 107.89 (CH), 70.47 ( $\text{CH}_2$ ), 67.74 ( $\text{CH}_2$ ), 59.16 ( $\text{CH}_3$ ), 37.2 ( $\text{CH}_2$ ); MS (FAB):  $m/z$  (%) = 896.5 (100) [ $\text{M}^+ + \text{H}$ ].

**6,13,20,27,34,41-Hexakis(2-methoxyethoxy)-all-homocalix[6](2,6)pyridine (10):** Yield: 0.03%; colourless solidified oil; TLC ( $\text{SiO}_2$ ):  $R_f = 0.5$  ( $\text{CH}_2\text{Cl}_2/\text{MeOH}/\text{conc NH}_3$  100:15:1);  $^1\text{H}$  NMR (200 MHz,  $\text{CDCl}_3$ ,  $25^\circ\text{C}$ ):  $\delta = 3.03$  (s, 24H;  $\text{CH}_2$ ), 3.41 (s, 18H;  $\text{OCH}_3$ ), 3.68 (m, 12H;  $\text{CH}_2$ ), 4.06 (m, 12H;  $\text{CH}_2$ ), 6.49 (s, 12H; Ar-H); MS (FAB):  $m/z$  (%) = 1075.6 (100) [ $\text{M}^+ + \text{H}$ ].

**2,6-Bis[2-(6'-methyl-2-pyridyl)ethyl]pyridine (11):** Yield: 0.8%; yellow solidified oil; TLC (SiO<sub>2</sub>):  $R_f = 0.72$  (CH<sub>2</sub>Cl<sub>2</sub>/MeOH/conc NH<sub>3</sub> 100:10:1); <sup>1</sup>H NMR (250 MHz, CDCl<sub>3</sub>, 25 °C):  $\delta = 2.54$  (s, 6H; CH<sub>3</sub>), 3.18 (s, 8H, CH<sub>2</sub>), 6.89–7.0 (m, 6H; Ar-H), 7.38–7.46 (m, 3H; Ar-H); <sup>13</sup>C NMR (62.9 MHz, CDCl<sub>3</sub>, 25 °C):  $\delta = 160.76$  (C), 160.67 (C), 157.83 (C), 136.55 (CH), 136.67 (CH), 120.67 (CH), 120.32 (CH), 119.89 (CH), 38.43 (CH<sub>2</sub>), 29.78 (CH<sub>2</sub>), 24.62 (CH<sub>2</sub>).

**2,6-Bis[1-(6'-methyl-2-pyridyl)-2-(6'-ethyl-2-pyridyl)ethyl]pyridine (12):** Yield: 0.7%; m.p. 152–153 °C; TLC (SiO<sub>2</sub>):  $R_f = 0.6$  (CH<sub>2</sub>Cl<sub>2</sub>/MeOH/conc NH<sub>3</sub> 100:10:1); <sup>1</sup>H NMR (250 MHz, CDCl<sub>3</sub>, 25 °C):  $\delta = 2.54$  (s, 6H; CH<sub>3</sub>), 3.18, 3.2 (s, 16H, CH<sub>2</sub>), 6.9–7.0 (m, 10H; Ar-H), 7.38–7.46 (m, 5H; Ar-H); <sup>13</sup>C NMR (62.9 MHz, CDCl<sub>3</sub>, 25 °C):  $\delta = 160.75$  (C), 160.64 (C), 157.82 (C), 136.60 (CH), 136.52 (CH), 120.70 (CH), 120.34 (CH), 119.91 (CH), 38.42 (CH<sub>2</sub>), 38.37 (CH<sub>2</sub>), 29.78 (CH<sub>2</sub>), 24.60 (CH<sub>3</sub>).

**1,2-Bis(4-methoxy-6-methyl-2-pyridyl)ethane (13):** Yield: 3%; m.p. 125 °C; TLC (SiO<sub>2</sub>):  $R_f = 0.7$  (CH<sub>2</sub>Cl<sub>2</sub>/MeOH/conc NH<sub>3</sub> 100:5:1); <sup>1</sup>H NMR (60 MHz, CDCl<sub>3</sub>, 25 °C, TMS):  $\delta = 2.46$  (s, 6H; CH<sub>3</sub>), 3.10 (s, 4H; CH<sub>2</sub>), 3.76 (s, 6H; OCH<sub>3</sub>), 6.50 (s, 4H; Ar-H); MS (FAB):  $m/z$  (%) = 273.2 (100) [ $M^+ + H$ ].

**Liquid–liquid extraction:** The extraction studies were performed at 25 ± 1 °C in 2 mL micro-reaction vials by means of mechanical shaking. The phase ratio  $V_{(org)}:V_{(w)}$  was 1:1 (0.5 mL each); the shaking time was 30 min. The extraction equilibrium was attained within a few minutes, except for Pd<sup>2+</sup> which required 2 h. The determination of the metal concentration in both phases was carried out radiometrically with the  $\gamma$ -radiation measurement of <sup>22</sup>Na, <sup>60</sup>Co, <sup>64</sup>Cu, <sup>65</sup>Zn, <sup>85</sup>Sr, <sup>109</sup>Pd, <sup>110m</sup>Ag, <sup>137</sup>Cs, <sup>198</sup>Au and <sup>203</sup>Hg in a NaI(Tl) scintillation counter (Cobra II, Canberra-Packard), and the  $\beta$ -radiation of <sup>115m</sup>Cd and <sup>204</sup>Tl in a liquid scintillation counter (Tricarb 2500, Canberra-Packard). The radioisotopes were supplied by Medgenix Diagnostics GmbH, Ratingen.

#### Liquid-membrane experiments:

**Membranes:** The ion-selective membranes consisted of almost 1% (wt/wt) of carrier dissolved in 33% (wt/wt), 66% (wt/wt) plasticiser dibutylsebacate and 0.6% (wt/wt) potassium tetrakis(chlorophenyl)borate as the anion blocker.

**Potentiometric measurements:** All measurements were carried out in cells of the following type: Ag; AgCl; KCl (3 M); LiOAc (0.1 M)/sample solution//membrane//internal electrolyte KCl (10<sup>-2</sup> M), AgCl; Ag. Potentiometric selectivity coefficients  $K_{ij}$  were determined by the separate solution method with 10<sup>-2</sup> M solutions of metal nitrates.

**Transport experiments:** Carrier-mediated transport of cations was studied in a coaxial cell in which two aqueous phases (source/receiving) are separated by a stirred chloroform membrane containing the carrier (5 × 10<sup>-4</sup> M). The aqueous source phase consisted of metal nitrates (5 × 10<sup>-2</sup> M); the receiving phase was deionised water. Transport without a carrier was carried out as a reference experiment (blank).

**Molecular modelling:** The molecular modelling studies were performed by DFT and ab initio calculations using Gaussian 94.<sup>[18]</sup> All calculations were carried out on a DEC 3000 AXP/800 workstation. CERIU<sup>2</sup> 1.6.2 was used for computer graphics and the initial building of the molecular models.

**Acknowledgments:** This work was supported by the Bundesministerium für Forschung und Technologie (Project NT20574). We thank Dr. D. Tieves and Dr. K. Wagemann (DECHEMA e.V., Frankfurt) for their cooperation. We are also obliged to Dr. S. Schuth and Dr. G. Eckhardt for recording the FAB-mass spectra.

Received: July 16, 1997 [F770]

- [1] F. Vögtle, J. Schmitz, M. Nieger, *Chem. Ber.* **1992**, *125*, 2523–2531; J. Schmitz, F. Vögtle, M. Nieger, K. Gloe, H. Stephan, O. Heitzsch, H.-J. Buschmann, W. Hasse, K. Cammann, *ibid.* **1993**, *126*, 2483–2491; J. Schmitz, F. Vögtle, M. Nieger, K. Gloe, H. Stephan, O. Heitzsch, H.-J. Buschmann, *Supramol. Chem.* **1994**, *3*, 115–119.
- [2] C. D. Gutsche, *Calixarenes, Monographs in Supramolecular Chemistry, Vol. 1* (Ed.: J. F. Stoddart), The Royal Society of Chemistry, Cambridge **1989**; J. Vicens and V. Böhmer (Eds.), *Calixarenes: A Versatile Class of Macrocyclic Compounds*, Kluwer Academic, Dor-

drecht **1991**; S. Shinkai, *Tetrahedron* **1993**, *49*, 8933–8968; V. Böhmer, *Angew. Chem.* **1995**, *107*, 785–818; *Angew. Chem. Int. Ed. Engl.* **1995**, *34*, 713–745.

- [3] E. Müller, G. Röscheisen, *Chem. Ber.* **1957**, *90*, 543–553.
- [4] J. Reedijk, in *Comprehensive Coordination Chemistry* (Ed.: G. Wilkinson), Pergamon, New York, **1987**, Vol. 2, pp. 976–978; E. C. Constable, *Metals and Ligand Reactivity*, VCH, Weinheim, **1996**; P. Tomasik, Z. Ratajczak, in *Pyridine–Metal Complexes* (Eds.: G. R. Newkome, L. Strekowski), Wiley-Interscience, New York, **1985**.
- [5] T. W. Bell, S. K. Sahni, in *Inclusion compounds: Key Organic Host Systems* (Eds.: J. L. Atwood, J. E. D. Davies, D. D. MacNicol), Oxford University Press, Oxford–New York–Tokyo, **1991**, pp. 325–390; T. Nabeshima, T. Inaba, T. Sagae, N. Furukawa, *Tetrahedron Lett.* **1990**, *31*, 3919–3922; Y. Okada, Y. Kasai, F. Ishii, J. Nishimura, *J. Chem. Soc. Chem. Commun.* **1993**, 976–978; O. Heitzsch, K. Gloe, H. Stephan, E. Weber, *Solvent Extr. Ion Exch.* **1994**, *12*, 475–496; K. Matsumoto, M. Hashimoto, M. Toda, H. Tsukube, *J. Chem. Soc. Perkin Trans 1* **1995**, 2497–2502; H. Sakamoto, S. Ito, M. Otomo, *Chem. Lett.* **1995**, 37–38.
- [6] F. Vögtle, G. Brodessa, M. Nieger, K. Rissanen, *Recl. Trav. Chim. Pays-Bas* **1993**, *112*, 325–329.
- [7] J. Gross, G. Harder, A. Siepen, J. Harren, F. Vögtle, H. Stephan, K. Gloe, B. Ahlers, K. Cammann, K. Rissanen, *Chem. Eur. J.* **1996**, *2*, 1585–1595.
- [8] The stoichiometry of the extracted species in two-phase distributions were determined by multiple regression analysis of the experimental data with a modified Marquardt procedure. See M. Petrich, L. Beyer, K. Gloe, P. Mühl, *Anal. Chim. Acta* **1990**, *228*, 229–234.
- [9] The usefulness of the DFT method is proven by calculation of the ligands and comparison with the X-ray structure.
- [10] The calculation of the charge density of the pyridine nitrogen with the DFT method gave markedly higher values for **3** and **7** compared with **1**.
- [11] K. Gloe, P. Mühl, J. Beger, *Z. Chem.* **1988**, *28*, 1.
- [12] K. Gloe, H. Stephan, R. Jacobi, J. Beger, *Solvent Extr. Res. Dev. (Japan)* **1995**, *2*, 18.
- [13] A suitable crystal was obtained by vapour diffusion of petroleum ether (40/60) into a solution of **3** and AgBF<sub>4</sub> in dichloromethane/acetonitrile. Crystal data: Enraf–Nonius CAD4 diffractometer; graphite monochromatised MoK $\alpha$  radiation ( $\lambda = 71.07$  pm); crystal dimensions: 0.18 × 0.20 × 0.25 mm, colourless, [C<sub>24</sub>H<sub>27</sub>N<sub>3</sub>O<sub>3</sub>Ag<sub>3</sub>(CH<sub>3</sub>CN)<sub>3</sub>][BF<sub>4</sub>]<sub>3</sub>,  $M = 1112.67$ , monoclinic,  $P2_1/c$  (No. 14),  $a = 986.8(1)$ ,  $b = 1582.1(3)$ ,  $c = 2559.3(4)$  pm,  $\beta = 95.06(1)^\circ$ ,  $V = 3.980(1)$  nm<sup>3</sup>,  $Z = 4$ ,  $\rho = 1.857$  g cm<sup>-3</sup>,  $\mu = 1.541$  mm<sup>-1</sup> (MoK $\alpha$ ),  $F(000) = 2184$ ; structure solution and refinement: 455 parameters, 7714 collected reflections, 6982 unique reflections ( $R_{int} = 0.027$ ), 2322 observed reflections [ $I > 3\sigma(I)$ ],  $R = 0.065$ ,  $R_w = 0.057$ ; weighting scheme:  $w = w'[1.0 - (\delta F/\sigma F)^2]$  ( $w' =$  Chebyshev polynomial for  $F_c$  with five coefficients: 2.57, -5.55, -0.0445, -1.68 and -1.50), largest difference peak (max.) = 0.90 e Å<sup>-3</sup>; data collection: scan type  $\omega/2\theta$ , scan range 0.85° + 0.34 tan $\theta$ ,  $T = 296 \pm 1$  K, index ranges  $2\theta_{max} = 50^\circ$ ,  $h: -11 \rightarrow 11$ ,  $k: 0 \rightarrow 18$ ,  $l: 0 \rightarrow 30$ . The structure was solved by direct methods (SHELXS<sup>[19]</sup>) and subjected to full-matrix refinement (CRYSTALS<sup>[20]</sup>). All non-H atoms, except B and F atoms, were refined anisotropically. The hydrogen atoms were calculated to their idealised positions with isotropic temperature factors ( $U = 0.08(\text{Å}^2)$ ) and included in the final structure factor calculations, but were not refined. Crystallographic data (excluding structure factors) for the structure reported in this paper have been deposited with the Cambridge Crystallographic Data Centre as supplementary publication no. CCDC-100756. Copies of the data can be obtained free of charge on application to CCDC, 12 Union Road, Cambridge CB2 1EZ, UK (fax: (+44) 1223-336033; E-mail: deposit@ccdc.cam.ac.uk).
- [14] Bond lengths: 207 pm (Ag1–N8), 218 pm (Ag2–N16), 217 pm (Ag3–N24); 211 pm (Ag1–N31), 209 pm (Ag2–N34), 213 pm (Ag3–N37). The adjacent acetonitrile nitrogen atoms N31 and N34 are separated by a distance of 335.5 pm. One BF<sub>4</sub><sup>-</sup> anion connects two silver atoms. The bond lengths of Ag2–F24–Ag3 are 260 and 259 pm, respectively.
- [15] The result of a search at the Cambridge Structural Data Centre.

- [16] See also Ag–Ag distances in other silver complexes: K. Hirotsu, I. Miyahara, T. Higuchi, M. Toda, H. Tsukube, K. Matsumoto, *Chem. Lett.* **1992**, 699–702; J. de Mendoza, E. Mesa, J.-C. Rodriguez-Ubis, P. Vázquez, F. Vögtle, P.-M. Windscheif, K. Rissanen, J.-M. Lehn, D. Lilienbaum, R. Ziessel, *Angew. Chem.* **1991**, *103*, 1365–1367; *Angew. Chem. Int. Ed. Engl.* **1991**, *30*, 1331–1333.
- [17] W. Hasse, B. Ahlers, J. Reinbold, K. Cammann, G. Brodesser, F. Vögtle, *Sens. Actuators B* **1994**, *18–19*, 380–382.
- [18] GAUSSIAN94, Revision B.2, Gaussian, Pittsburgh, PA, **1995**.
- [19] G. M. Sheldrick, in *Crystallographic Computing 3* (Eds.: G. M. Sheldrick, C. Krüger, R. Goddard), Oxford University Press, Oxford (UK), **1985**, pp. 175–189.
- [20] D. Watkin, J. R. Carruthers, P. W. Betteridge, *Crystals*, Chemical Crystallography Laboratory, Oxford (UK), **1990**.
-